Journal of Materials Chemistry A

Accepted Manuscript

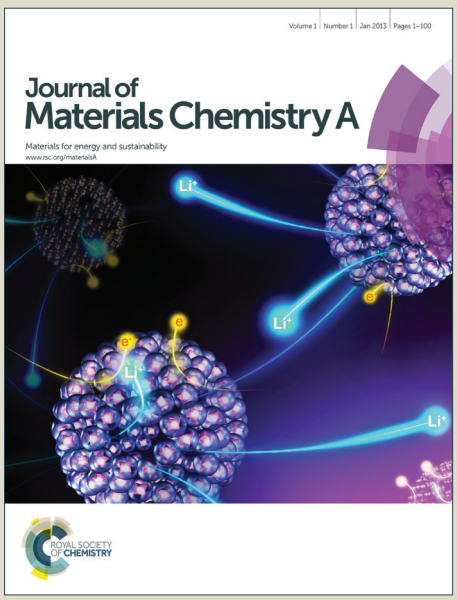

ROYAL SOCIETY OF CHEMISTRY

www.rsc.org/materialsA

Journal Name RSCPublishing

Cite this: DOI: 10.1039/x0xx00000x

A Facile Approach to Prepare Porphyrinic Porous Aromatic Frameworks for Small Hydrocarbons Separation

Shuang Meng, Heping Ma, Lingchang Jiang, Hao Ren, Guangshan Zhu*

Received 00th January 2012,
Accepted 00th January 2012

DOI: 10.1039/x0xx00000x

www.rsc.org/

Porous organic frameworks (POFs) have attracted a great deal of attention thanks to their high surface areas, high stability and controllable skeletons. We synthesize series of porphyrin-based porous aromatic frameworks (PAF-40s) in a cost-effective approach. The PAF-40s exhibit high surface area, excellent chemical and thermal stability. Specifically, these PAFs materials possess high adsorption capacity of small hydrocarbons, such as methane, ethylene, ethane and propane, at room temperature. Futuremore, the PAFs have remarkably high adsorption selectivity values of C_2 and C_3 hydrocarbons over CH_4.

Introduction

Porous materials have diverse potential applications in the areas of molecular capture and storage[1], gas separations[2], as catalyst[3,4]. Recently, porous organic polymers (POPs)[5-9] consisting of purely organic building-block networks, such as covalent organic frameworks (COFs)[10,11], polymers of intrinsic microporosity (PIMs)[12,13], covalent triazine-based frameworks (CTFs)[14.15], conjugated microporous polymers (CMPs)[16-18] and porous aromatic frameworks (PAFs)[19-21], have attracted a great deal of attention thanks to their high surface areas, high stability and controllable skeletons. The emergence of POPs provides a new class of porous materials with rigid aromatic open-framework structure constructed by covalent bonds. Nowadays, the research of POPs concerning the structure design, synthesis method and intriguing properties have been widely studied. It has been documented that the polymerization reactions using the expensive and rare transition/noble metal catalyst are effective strategies to construct POP materials. In addition, the reactions are mostly carried out under anhydrous and inert conditions. Accordingly, POPs with versatile structures and fascinating properties have rarely been applied to practical production, which is limited by mass production. There is no doubt that it is greatly useful to explore a cost-effective approach to prepare POPs with excellent pore property.

Porphyrin is a kind of diverting macrocycle and the centered square-planar offers rich coordination site for many metal ions, such as Mn, Fe, Al, Zn, etc. Very recently, we reported a series of Porphyrinic-CTF materials[22] synthesized under ionothermal condition using $ZnCl_2$ as catalysis. Interestingly, the Zn ions could be also combined into the porphyrin center. More valuably, porphyrin and its derivatives with well-defined planar and rigid structure have been developed for synthesis of porous materials[23-25].

It is obvious that the functional groups (such as -Br, -CN, $-B(OH)_2$) are critically demanded for synthesis of POP materials. In our recent research, we try our best to seek cost-effective approach to synthesize PAFs. By using Lewis acid $AlCl_3$ as catalysis, the aromatic phenyl rings could couple directly. Herein, we report the synthesis and properties of a series of porphyrin-based porous organic frameworks based on 5,10,15,20-Tetraphenylporphyrin and its metelloporphyrins (Mn, Fe) materials. The resulting PAFs, denoted as PAF-40, PAF-40-Mn, and PAF-40-Fe, exhibit high surface area, high thermal and chemical stabilities. Furthermore, they show high adsorption capacity of small hydrocarbons (CH_4, C_2H_4, C_2H_6 and C_3H_8) at room temperature. More valuably, PAFs have remarkably high adsorption selectivity of C_2 and C_3 hydrocarbons over CH_4.

The separation of natural gas is important in energy and petroleum chemistry related domains since different components in natural gas are utilized for different purposes. Thus, the study on improved separation and purification of the small hydrocarbons will lead to vital reduction in energy requirements and costs[26-29]. At present, the pressure swing adsorption (PSA) [30] process has been successfully developed as a cost-effective and highly efficient technique for separating small hydrocarbons from their mixture. In the PSA process, solid adsorbents with specific adsorption properties influence basically the separation efficiency. Thus, the development of solid adsorbents, such as zeolites, activated carbons, metal organic frameworks (MOFs) and POPs, meet this great challenge for PSA technology. It has been proved that porous

materials with small pore sizes is befitting for small hydrocarbons capture.

Experiment

Materials

All starting materials (Porphyrin, $FeCl_2$, $MnCl_2$, $AlCl_3$, Chloroform, Tetrahydrofuran and Hydrochloric acid) were purchased from commercial suppliers and used without further purification unless otherwise noted. Synthesis of 5,10,15,20-Tetraphenylporphyrin, 5,10,15,20-Tetraphenylporphyrin-Fe and 5,10,15,20-Tetraphenylporphyrin-Mn were based on the previously reported method[31].

Synthesis of PAF-40

5,10,15,20-Tetraphenylporphyrin (385mg, 0.62 mmol) and $AlCl_3$ (1.600 g, 4.5 mmol) were put into a 100 mL 2-neck dried flask .Then a condenser and a magnetic stirring bar were added into the flask. After degassing by Ar gas, dried $CHCl_3$ (40 mL) was added to the flask and the mixture was heated to 60 ^oC for 42 h under an inert atmosphere. After cooling to room temperature, the crude product was collected by filtration and washed with ethanol, HCl (3 M) and methanol. Further purification of PAF-40 was carried out by Soxhlet extraction with methanol and THF for 24 h, respectively. The product was dried in vacuum at 120 ^oC to give PAF-40 as a black powder. Synthesis of PAF-40-Mn and PAF-40-Fe are in a similar procedure shown in supporting information.

Instruments

The Thermogravimetric Analysis (TGA) was performed using a Netzch Sta 449c thermal analyzer system at the heating rate 10 ^oC/min in air atmosphere. The Inductive Coupled Plasma (ICP) analysis was measured using a Perkin Elmer Optima 3300DV. The Elemental analysis (for C, H, N) were measured using a Perkin Elmer 2400 Series II CHNS/O Analyzer. The FTIR spectra were measured using a Nicolet Impact 410 Fourier transform infrared spectrometer. The nitrogen adsorption isotherms were measured on a Quanta Autosorb-1c analyzer. The XRD was performed by a Rigaku D/max 2500 diffractometer using CuKα radiation, 40 kV, 200 mA with scanning rate of 0.3° min^{-1} (2θ). Scanning Electron Microscopy (SEM) was recorded using a JEOL JEM 6700. Transmission Electron Microscopy (TEM) was recorded using a JEOL JEM 3010. The solid–state 13C NMR was performed by a Bruker Avance 400MHz Solid-State NMR Spectrometer.

Results and discussion

Currently, the synthesis of porphyrin based porous materials has been greatly developed thanks to the macrocycle structure of porphyrin offering rich coordination site for different metal ions, such as Mn, Fe, Al, Zn, etc. To obtain the porphyrin based POPs, the monomers should have the functional groups, such as -Br, -CN, $-B(OH)_2$, etc. Inspired by the successful synthesis of PAFs through Lewis acid $AlCl_3$ triggered aromatic phenyl rings coupling reaction, a series of porphyrin based PAFs are synthesized by this cost-effective and facile approach.

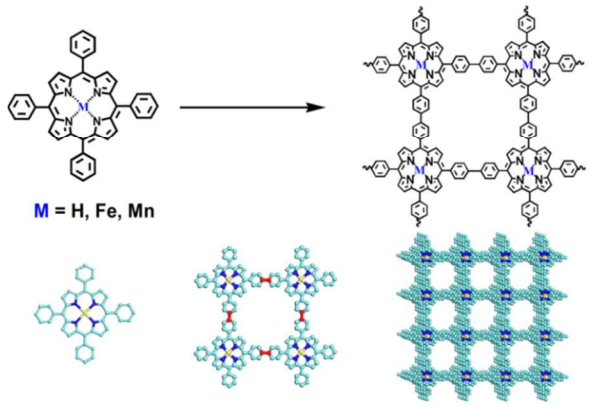

Figure 1. Schematic representation of the synthesis of the PAF-40, PAF-40-Fe and PAF-40-Mn.

As shown in Figure 1, 5,10,15,20-Tetraphenylporphyrin, its metelloporphyrins (Mn, Fe) are selected as the original monomers. For metelloporphyrins, the Mn and Fe ions are previously occupied the porphyrin center.

The reaction process was monitored by FT-IR analysis of the PAF samples and corresponding initial monomers (Figure S1-S3). When the coupling reaction occurs, the position and absorbance of C-H and C-C vibrations for benzene ring in the range of 1650-1400 cm^{-1} and 800-700 cm^{-1} are shifting to lower wavenumbers and decreasing respectively. Another peak near 800 cm^{-1} is observed as well in the product, which is ascribed to para-substituted benzene ring. This evidence points that benzene rings are coupled together to form an extended network. In addition, the metal-porphyrin characteristic vibration of 1001 cm^{-1} corresponding to the absorbance of Fe–N and Mn–M bonds[29] suggests that the metal cations are encapsulated in Metelloporphyrin of PAF-40-Fe and PAF-40-Mn networks (Figure S2 and Figure S3).

For better illustration of the local structures of the polymers, solid-state ^{13}C NMR was carried out. As shown in Figure S5 Figure S6 and Figure S7 the signal of carbon around 128 and 137 ppm is observed, which could be assigned to carbon in the benzene ring. The carbon signals assigned to porphyrin are also detected around 118 and 153 ppm in the spectrum. The skeletal structure is as expected.

The contents of PAF-40s for the metal ions of Al, Fe and Mn measured by inductively coupled plasma (ICP) spectroscopy give a supporting proof that these ions are encapsulated in the PAF skeletons (Table S2). As can be seen from the data, three polymers have aluminium element, the considerable amounts of aluminium derived from the reaction catalyst-$AlCl_3$. Residues of aluminum in framework may affect the pore size distribution and increase the interpenetrating effect, thereby affecting the adsorption of gas at a certain extent.

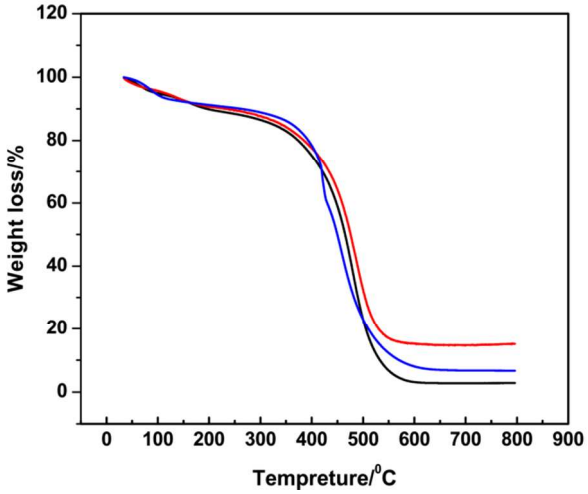

Figure 2. TGA plots of PAF-40 (black), PAF-40-Fe (red), and PAF-40-Mn (blue) in air atmosphere.

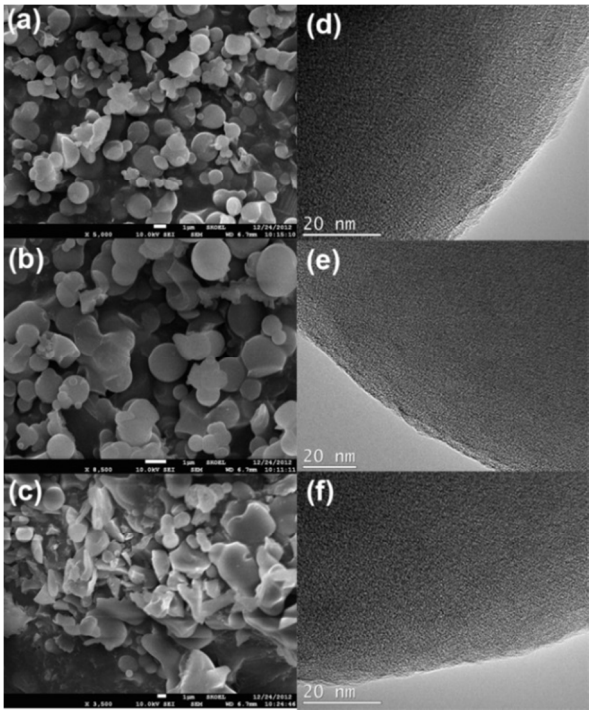

Figure 3. SEM images of PAF-40 (a), PAF-40-Fe (b) and PAF-40-Mn (c); TEM images of PAF-40 (d), PAF-40-Fe (e) and PAF-40-Mn (f).

Thermogravimetric analysis (TGA) curves collected under air condition are shown in Figure 2. Small weight loss is observed below 200 ^{o}C due to the removal of occluded solvents. The organic moieties in the frameworks start to be decomposed around 400 ^{o}C, indicating prepared PAF-40 materials have high thermal-stability. The amorphous nature of PAF-40, PAF-40-Fe and PAF-40-Mn in structure is proven by the X-ray powder diffraction measurement (Figure. S4). The morphologies of PAF-40 particles are visualized by scanning electron microscopy (SEM) and transmission electron microscopy (TEM). The images in Figure 3 show that the shape of particles is irregular lamella and the particle size is around 100 nm.

The pore characters of PAF-40, PAF-40-Fe, PAF-40-Mn were investigated by nitrogen sorption measurement at 77 K. As indicated in Figure 4, they show type I isotherm featured by a sharp uptake at the low-pressure region. Adopting the Langmuir model to the low-pressure region of the isotherm, the surface area was 601 m^2 g^{-1}, 668 m^2 g^{-1} and 827 m^2 g^{-1}, respectively. The apparent surface areas were also calculated from the Brunauer–Emmett–Teller (BET) model.

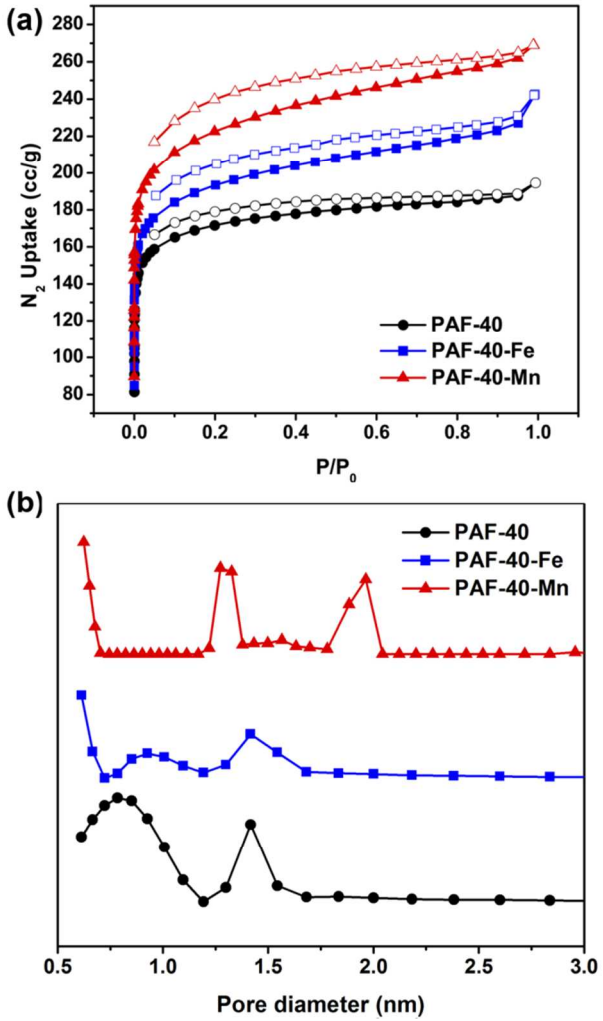

Figure 4. (a) Nitrogen adsorption and desorption isotherms measured at 77 k for PAF-40 (black), PAF-40-Fe (blue), PAF-40-Mn (red); (b) Pore size distribution of PAF-40 (black), PAF-40-Fe (blue) and PAF-40-Mn (red). PSD is calculated by the NLDFT method.

Journal Name RSCPublishing

Table 1. The BET surface areas, pore volume, pore diameter and isosoteric heats of adsorption for PAF-40, PAF-40-Fe, PAF-40-Mn.

PAFs	BET [m^2/g]	Pore volume [cc/g]	QstCH_4 [kJ/mol]	QstC_2H_4 [kJ/mol]	QstC_2H_6 [kJ/mol]
PAF-40	601	0.266	18.2	24.7	36
PAF-40-Fe	628	0.337	23.1	30	47.8
PAF-40-Mn	827	0.406	15.5	25.1	34.8

It is mentioned that PAF-40-Mn has higher surface area than the others, owning to its initial monomer has better solubility. With the introduction of Fe and Mn elements, so that the solubility of the monomers improved, the degree of polymerization of the reaction enhanced, the order of the skeleton increased.So we can see the different nitrogen sorption caused by metal content. The pore size distributions of PAFs were calculated by the nonlocal density functional theory (NLDFT) method. These products displayed main pore size distribution below 2 nm. For clear illustration, the pore parameters derived from the nitrogen isotherms are listed in table 1.

Given the aromatic framework of PAF-40 products together with their narrow and small PSDs, their small hydrocarbons adsorptions are evaluated. The CH_4, C_2H_4 and C_2H_6 isotherms were measured at 273 K (Figure S8, Figure S9 and Figure S10) and 298 K (Figure 5), respectively. For clear illustration, the capacities of small hydrocarbons are listed in table 2. It is clear that these PAF materials can adsorb more C_3H_8, C_2H_6, C_2H_4 than CH_4.

For example, at 298 K, PAF-40-Fe can adsorb large amounts of C_3H_8, C_2H_6 and C_2H_4, with values of 57.9 cc/g, 41.4 cc/g and 51.8 cc/g, respectively, which is nearly five, three and four times than CH_4 (13.8 cc/g). It is notable that the adsorption of C_3H_8 is larger at the low pressure.

For better understanding their affinity with probe molecules, the isosteric heats of adsorption (Qst) of PAF-40 materials are calculated based on the adsorption isotherms at 273 K and 298 K and corresponding fittings based on the Virial equation. As shown in Figure 6, PAF-40, PAF-40-Fe and PAF-40-Mn have notably high Qst values for these small hydrocarbons (C_2H_6: 36 kJ/mol, 47.8 kJ/mol, 34.8 kJ/mol; C_2H_4: 24.7 kJ/mol, 30 kJ/mol, 25.1 kJ/mol; CH_4: 21.8 kJ/mol, 23.1 kJ/mol, 23.9 kJ/mol). It worth mentioning that the heat of adsorption for CH_4 of PAF-40-Mn is close to the value of PCN-14, which is up to 30 kJ/mol[32]. The Qst of C_2H_6 is higher than CH_4 and C_2H_4, and the Qst of CH_4 is lowest. The strong interaction between the host and gas molecules could be attributed to uniform micropores in the framework, which increases the Van der Waals forces between the C_2H_6 molecules. On the other hand, the introduction of metal is also the vital reason for the excellent adsorption capacity.

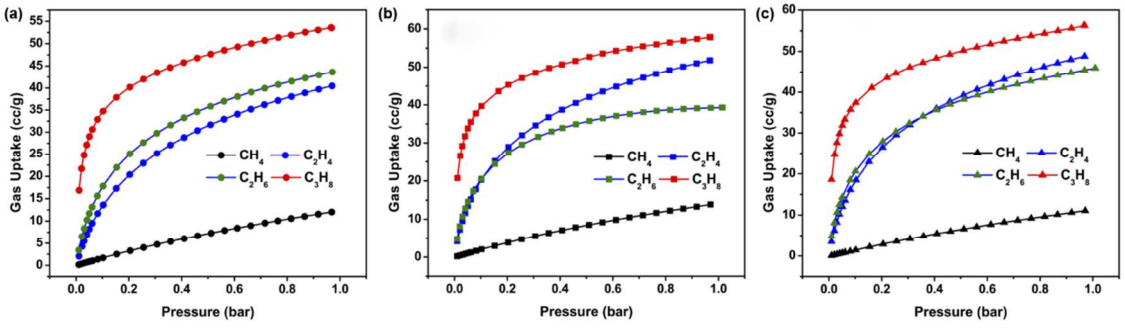

Figure 5. Gas uptake isotherms (CH_4 black, C_2H_4 red, C_2H_6 blue, C_3H_8 olive) for PAF-40 (a), PAF-40-Fe (b) and PAF-40-Mn (c) at 298 k

Journal Name RSCPublishing

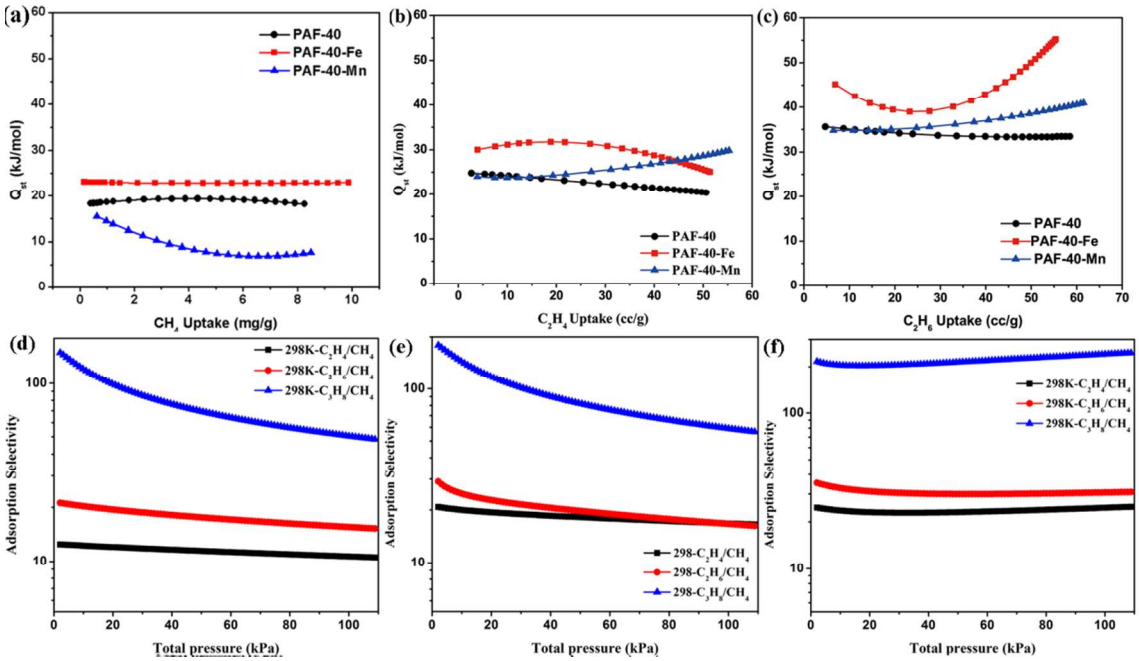

Figure 6. The isosteric heats of adsorption of PAF-40, PAF-40-Fe and PAF-40-Mn for CH_4 (a), C_2H_4 (b) and C_2H_6 (c), respectively. IAST-predicted adsorption selectivity of PAF-40 (d) , PAF-40-Fe (e) and PAF-40-Mn (f) at 298K and 110kPa.

Table 2. The adsorption and selectivity of CH_4-C_2H_4, CH_4-C_2H_6 and CH_4-C_3H_8 for PAF-40, PAF-40-Fe and PAF-40-Mn.

PAFs	CH_4[a]	CH_4[b]	C_2H_4[a]	C_2H_4[b]	C_2H_6[a]	C_2H_6[b]	C_3H_8[a]	C_3H_8[b]	C_2H_4/CH_4[a]	C_2H_6/CH_4[a]	C_3H_8/CH_4[a]
PAF-40	12.0	18.8	40.4	50.3	43.6	58.0	53.6	63.0	10.5	15.2	48.2
PAF-40-Fe	13.8	24.1	51.8	56.1	41.4	66.9	57.9	51.2	16.1	16.2	56
PAF-40-Mn	11.0	27.0	48.8	52.3	45.9	63.5	56.3	60.8	24.9	30.8	246

[a] T=298 K, P= 110kPa. [b] T=273 K.

Besides the loading capacity, the adsorption selectivity of porous solid materials for binary gas mixtures is another key parameter to evaluate the potential of gas separation. The adsorption selectivities of PAF-40 materials for C_2H_4, C_2H_6 and C_3H_8 over CH_4 were estimated by IAST theory[33] (Figure 6 and Figure S13-15). As illustrated in table 2 and Figure 6, PAF-40 materials show high selectivity for C_2H_4 over CH_4, C_2H_6 over CH_4 and C_3H_8 over CH_4. At 298K, 110 kPa, the C_2H_4/CH_4, C_2H_6/CH_4 and C_3H_8/CH_4 selectivities on PAF-40 are 10.5, 15.2 and 48.2 respectively. The selectivity of C_2H_4, C_2H_6 and C_3H_8 over CH_4 for PAF-40-Fe and PAF-40-Mn is higher than that of PAF-40. At the same condition, the selectivities of C_2H_4/CH_4, C_2H_6/CH_4 and C_3H_8/CH_4 for PAF-40-Fe is 16.1, 16.2 and 56; the selectivity of C_2H_4, C_2H_6 and C_3H_8 over CH_4 for PAF-40-Mn reach 24.9, 30.8 and 246, respectively. And at 273K, the C_2H_4/CH_4, C_2H_6/CH_4 and C_3H_8/CH_4 selectivities of PAF-40, PAF-40-Fe and PAF-40-Mn are shown in Figure S13-15. It can be seen the materials possessing metal site have better separation effect for C_2, C_3 hydrocarbons over CH_4 at room temperature. This is because that the exposed metal sites in the skeleton increased the adsorption interaction between C_2, C_3 hydrocarbons and the porous framework.

Overall, our experimental results show that the adsorption capacity of these polymers for small hydrocarbons follows the trend of C3 > C2 > C1. In addition, these PAF materials have high isosteric heats of adsorption (Qst) for small hydrocarbons. Moreover, from another perspective, the trend of gas adsorption capacity and separation selectivity as follows: PAF-40-Mn > PAF-40-Fe > PAF-40-Al. Thus, we have proved that

immobilization of metal ions in our polymers has great value of improving gas selection selectivity (Table S3).

Conclusions

In summary, we have successfully synthesized a series of porphyrinic porous aromatic frameworks triggered by $AlCl_3$ coupling reaction, which are microporous solid confirmed by nitrogen sorption. The preparation method is quite facile and cheap since $AlCl_3$ was used as the catalyst. Screening the catalysts employed for POF materials, very expensive catalysts or sophisticated process were generally used in the condensation reaction, for example Pd catalyst or $ZnCl_2$ under a high temperature (>400°C) and high pressure. Meanwhile, the porphyrin-based porous organic frameworks were synthesized under a mild condition (heat to 60°C) to achieve the same polymerization effect. In addition, PAF-40 materials show higher adsorption capacity for the C_2H_4, C_2H_6 and C_3H_8 than CH_4. Moreover, they also exhibit a significantly high selectivity for C_3H_8 over CH_4 and high selectivities for C_2H_6 and C_2H_4 over CH_4, respectively. The high sorption performance and selectivity of PAF-40 materials promise greatly potential for energy efficient separation of small hydrocarbons.

Acknowledgements

We are grateful to the financial support from National Basic Research Program of China (973 Program, grant nos.2012CB821700), Major International (Regional) Joint Research Project of NSFC (grant nos. 21120102034) and NSFC (21201074).

Notes and references

State Key laboratory of Inorganic Synthesis & Preparative Chemistry, Jilin University, Changchun, 130012, P. R. China
To whom correspondence should be addressed: E-mail: zhugs@jlu.edu.cn. Fax: +86-431-85168331; Tel: +86-431-85168331.

Electronic Supplementary Information (ESI) available: [details of any supplementary information available should be included here]. See DOI: 10.1039/b000000x/

1. S. Choi, J. H. Drese and C. W. Jones, *ChemSusChem.*, 2009, **2**, 796-854.
2. J. R. Li, R. J. Kuppler and H. C. Zhou, *Chem. Soc. Rev.*, 2009, **38**, 1477-1504.
3. J. Perez-Ramirez, C. H. Christensen, K. Egeblad, C. H. Christensen and J. C. Groen, *Chem. Soc. Rev.*, 2008, **37**, 2530-2542.
4. P. Kaur, J. T. Hupp and S. T. Nguyen, *ACS Catal.*, 2011, **1**, 819-835.
5. B. Kesanli and W. Lin, *Coord. Chem. Rev.*, 2003, **246**, 305-326.
6. D. Wu, F. Xu, B. Sun, R. Fu, H. He and K. Matyjaszewski, *Chem. Rev.*, 2012, **112**, 3959-4015.
7. S. L. James, *Chem. Soc. Rev.*, 2003, **32**, 276.
8. R. Dawson, A. I. Cooper and D. J. Adams, *Prog. Polym. Sci.*, 2012, **37**, 530-563.
9. X. Zou, H. Ren and G. Zhu, *Chem. Commun*, 2013, **49**, 3925-3936.
10. S. Y. Ding and W. Wang, *Chem. Soc. Rev.*, 2013, **42**, 548-568.
11. A. P. Cote, A. I. Benin, N. W. Ockwig, M. O'Keeffe, A. J. Matzger and O. M. Yaghi, *Science*, 2005, **310**, 1166-1170.
12. N. B. McKeown and P. M. Budd, *Macromolecules*, 2010, **43**, 5163-5176.
13. N. B. McKeown and P. M. Budd, *Chem. Soc. Rev.*, 2006, **35**, 675-683.
14. P. Kuhn, M. Antonietti and A. Thomas, *Angew. Chem., Int. Ed.*, 2008, **47**, 3450-3453.
15. M. J. Bojdys, J. Jeromenok, A. Thomas and M. Antonietti, *Adv. Mater.*, 2010, **22**, 2202-2205.
16. A. I. Cooper, *Adv. Mater.*, 2009, **21**, 1291-1295.
17. R. Dawson, A. Laybourn, R. Clowes, Y. Z. Khimyak, D. J. Adams and A. I. Cooper, *Macromolecules*, 2009, **42**, 8809-8816.
18. F. S. Jia-Xing Jiang, Abbie Trewin, Colin D. Wood, Hongjun Niu, and Y. Z. K. James T. A. Jones, and Andrew I. Cooper, *J. Am. Chem. Soc.*, 2008, **130**, 7710-7720.
19. T. Ben, H. Ren, S. Ma, D. Cao, J. Lan, X. Jing, W. Wang, J. Xu, F. Deng, J. M. Simmons, S. Qiu and G. Zhu, *Angew. Chem., Int. Ed.*, 2009, **48**, 9457-9460.
20. H. Ren, T. Ben, E. Wang, X. Jing, M. Xue, B. Liu, Y. Cui, S. Qiu and G. Zhu, *Chem. Commun.*, 2010, **46**, 291-293.
21. H. Zhao, Z. Jin, H. Su, X. Jing, F. Sun and G. Zhu, *Chem. Commun.*, 2011, **47**, 6389-6391.
22. H. Ma, H. Ren, S. Meng, F. Sun and G. Zhu, *Sci. Rep.*, 2013, **3**, 2611.
23. N. B. McKeown, S. Hanif, K. Msayib, C. E. Tattershall and P. M. Budd, *Chem. Commun.*, 2002, 2782-2783.
24. L Chen, Y Yang and D Jiang, *J. Am. Chem. Soc.*, 2010, **132**, 9138-9143.
25. A. M. Shultz, O. K. Farha, J. T. Hupp and S. T. Nguyen, *Chem. Sci.*, 2011, **2**, 686.
26. Y. He, Z. Zhang, S. Xiang, F. R. Fronczek, R. Krishna and B. Chen, *Chem. Commun.*, 2012, **48**, 6493-6495.
27. A. P. Katsoulidis and M. G. Kanatzidis, *Chem. Mater.*, 2012, **24**, 471-479.
28. H. J. Mackintosh, P. M. Budd and N. B. McKeown, *J. Mater. Chem.*, 2008, **18**, 573.
29. J. K. Stolaroff, S. Bhattacharyya, C. A. Smith, W. L. Bourcier, P. J. Cameron-Smith and R. D. Aines, *Environ. Sci. Technol.*, 2012, **46**, 6455-6469.
30. H. Järvelin and J. R. Fair, *Ind. Eng. Chem. Res*., 1993, 32,2201–2207.
31. P. J. F. Gauuan, M. P. Trova, L. G.-Boros, S. B. Bocckino, J. D. Crapo and B. J. day, *Bioorg. Med. Chem.*, 2002, **10** 3013-3021.
32. S. Ma, D. Sun, J. M. Simmons, C. D. Collier, D. Yuan and H. Zhou, *J. Am. Chem. Soc.,* 2008, **130**, 1012-1016.
33. J. Chen, L. S. Loo and K. Wang, *J. Chem. Eng. Data.*, 2011, **56**, 1209-1212.